Two-dimensional supramolecular self-assembly probed by scanning tunneling microscopy

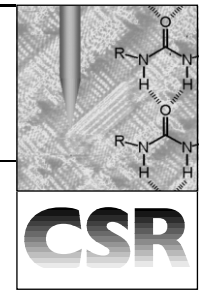

Steven De Feyter* and Frans C. De Schryver

Katholieke Universiteit Leuven, Department of Chemistry, Celestijnenlaan 200 F, B-3001 Heverlee, Belgium

Received 8th January 2003
First published as an Advance Article on the web 2nd April 2003

Supramolecular chemistry has a very large impact on chemistry of current interest and the use of non-covalent but directional forces is appealing for the construction of ′supramolecular architectures′. The invention of scanning probe microscopy techniques has opened new doorways to study these concepts on surfaces. This review deals with recent progress in the study of two-dimensional supramolecular self-assembly on surfaces probed by scanning tunneling microscopy, with a special emphasis on structure, dynamics and reactivity of hydrogen bonded systems.

1 Introduction

Nanoscience and nanotechnology are just emerging and a great deal of effort is being spent to make them become reality as they have great potential to have a significant impact on our society. Surface science plays a crucial role as all (nano)(electronic)devices made will most likely need to be supported on a surface. Templating surfaces in a controlled way will therefore be very important. Many different approaches exist but it is generally recognised that the effective rational handling of nano-size entities will, ultimately, require the advancement of a 'bottom-up' chemical approach. Self-assembly, which is the spontaneous formation of highly organised functional supramolecular architectures, will be of great value. Supramolecular chemistry, defined as the chemistry beyond the chemical bond, has taught us how to exploit non-covalent bonds to make controlled structures.[1] However, the concept of using selective and directional non-covalent interactions has been applied mostly in solution and in crystals.[2,3] In two dimensions, at surfaces, these concepts have not been fully exploited yet and it is only over the past few years that this particular field of research has boomed, thanks to the invention of scanning probe techniques. This research is motivated by the quest to understand the factors ruling the supramolecular ordering in two dimensions in order to control the outcome of the self-assembly process itself.

In this contribution we will review the progress in controlling the supramolecular ordering of molecules of (sub)monolayer covered films on solid surfaces as investigated by scanning tunneling microscopy (STM), which is the technique of choice to study these systems. This review mainly deals with those molecular systems which by physisorption or very weak forces interact with the substrate and which display directional non-covalent interactions (mainly but not exclusive hydrogen bonding). The rich chemistry and supramolecular aspects of so-called self-assembled monolayers, *e.g.* thiols on gold, will not be covered.[4,5]

2 Scanning tunneling microscopy

The invention of the STM in the early eighties[6] opened new ways to investigate surface phenomena on a truly atomic scale thanks to the very localised nature of the probing. In STM, a metallic tip is brought very close to a conductive substrate and by applying a voltage between both conductive media, a tunnelling current may result. The exponential distance dependence of the tunnelling current provides excellent means to

Steven De Feyter (Kortrijk, Belgium, 1971) is a postdoctoral researcher in the group led by Prof. Frans De Schryver at the Katholieke Universiteit Leuven in Belgium. After working on scanning tunnelling microscopy during his PhD in this group he moved to a postdoctoral position in Prof. Ahmed Zewail's group (California Institute of Techonoly, Pasadena) where he was involved in ultrafast organic femtochemistry. He rejoined the Leuven group in 1999. His current interests include the study of supramolecular chemistry and self-assembly phenomena at surfaces with scanning probe methods.

Frans De Schryver (St-Niklaas, Belgium, 1939) is full professor at the Katholieke Universiteit Leuven where, since a postdoctoral stay with Prof. C. Marvel in 1969, he has been involved in the study of excited states of organic synthetic systems. His present research activities combine fundamental photophysical methodologies, such as time resolved spectroscopy, with space resolution down to the single molecule level. He has received the Alexander von Humboldt (1993) and Max Planck (2001) Awards as well as the Porter Medal (1998).

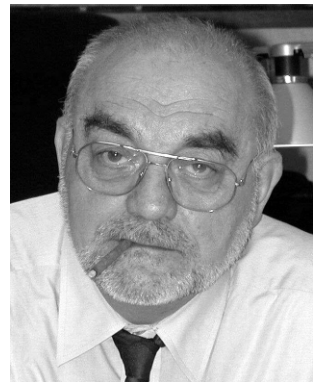

control the distance between the probe and the surface and very high resolution (atomic) on atomic flat conductive substrates can be achieved. The initial applications of STM dealt with imaging of semiconductor, inorganic and metal surfaces and later on, the first experiments on molecules adsorbed on surfaces were reported. The method requires conductive substrates, immobilisation of the molecules and due to the distance dependence of the tunneling process, only very thin layers—typically monomolecular—can be probed.

The first experiments on molecular adlayers were carried out under ultrahigh vacuum (UHV) conditions on metal surfaces.[7] Provided that the chemisorption energy is high enough on atomically flat conducting metal and semi-conductor surfaces, individual molecules can be visualised. To overcome the problem of molecular mobility for those systems with too weak adsorbate–substrate interactions, two approaches have been followed: 1) controlling the temperature under UHV conditions and 2) the formation of two-dimensional (2D) adlayers. In addition, the presence of certain functional groups (vide infra) can help in stabilizing the monolayer via intermolecular interactions (*e.g.* hydrogen bonding) or adsorbate–substrate interactions (*e.g.* alkyl chains on highly oriented pyrolytic graphite (HOPG)). Control of the mobility of molecules at room temperature really allows advantage to be taken of the versatility of STM to operate at the interface between two condensed media, one being an atomically flat conducting solid and the other being a gas or a liquid or a liquid crystalline material or a gel.

Note that high-resolution STM imaging requires immobilisation of the molecules but that very strong adsorbate-substrate interactions are not favourable for the formation of highly structured supramolecular structures. Self-organisation requires that molecules upon deposition on a substrate can rotate and translate to 'find' each other in order to form the thermodynamically most stable supramolecular ordering at a given temperature.

Due to the nature of the tunneling process, the substrate has to be conducting. Preferentially, it should also be atomically flat. Under UHV conditions, several metal and semi-conductor surfaces have been used as support. Organic molecular beam epitaxy (OMBE) is the method of choice to deposit molecules under UHV conditions.[8]

Under atmospheric conditions at room temperature, the first report on molecular imaging at the solid–fluid interface was on a liquid-crystalline compound on HOPG.[9] HOPG is the most popular substrate to work with under ambient conditions: it is electrically conductive, atomically flat, inert and is easy to clean. Moreover, alkylated compounds have a high affinity for this substrate. The thickness of the film is not critical since the tip penetrates through the excess insulating organic material. Also liquid-like organic compounds or isotropic organic solutions allow STM imaging.[10,11] Monolayers form spontaneously by physisorption and stable imaging is achieved if the molecules are laterally immobilised by adsorbate–adsorbate and adsorbate–substrate interactions. The formation of monolayers at the solid–liquid interface can also be induced under potential control.[12] The electrochemical method utilises an electric potential to increase the affinity of the adsorbates to the conductive substrates. Spin coating or drop casting of diluted solutions allows imaging at the solid–air interface.[13] Other approaches include transfer of films at the water–air interface to the substrate by means of the Langmuir–Blodgett technique (vertical dipping)[14] or the horizontal lifting method.[15] Not all compounds have a high enough affinity for the substrate to allow immobilisation at room temperature. Some approaches take advantage of the formation of mixed adlayers: molecules can be stabilised by adsorption on top of a 'buffer' layer if the buffer layer has a higher affinity for the substrate than the molecule of interest and if as a result the molecule of interest has a lower mobility upon adsorption on the buffer layer than on the substrate.[16] Alternatively, molecules can also be stabilised by co-adsorption with other molecules.[7]

UHV conditions provide a well-defined environment with control of the substrate coverage. In addition, temperature control gives a handle to control the mobility of the molecules and as such individual molecules, clusters, one-dimensional (1D) rows and 2D patterns can be deposited. However, not all species can be adapted to UHV conditions, such as those with relatively low thermal stability. The technical challenges are less severe under ambient conditions and in-situ imaging is possible.

3 Monocomponent supramolecular structures

The self-assembly of molecules to form well-defined supramolecular structures under the influence of weak forces such as hydrogen bonding, electrostatic interactions, and hydrophobic interactions have been discussed in detail in solution and in three-dimensional (3D) crystals.[1,3,17] In this part, we focus on selected examples of monocomponent supramolecular architectures formed on surfaces by directional but weak interactions.

A substantial number of systems have been investigated at the solid–liquid interface where hydrogen bonding plays an important role in the formation and the structure of 2D monolayers: these systems include monoalkylated long-chain alcohols,[18] fatty acids, and amines to name a few (Fig. 1).[19]

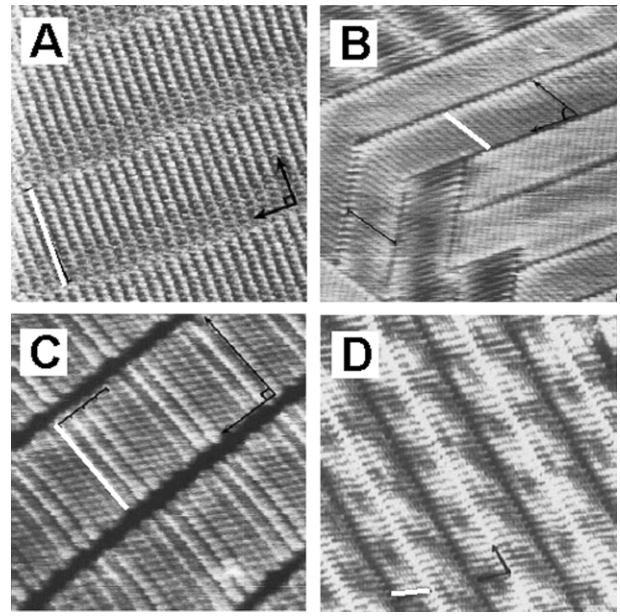

Fig. 1 STM image of (A) triacontane ($CH_3(CH_2)_{28}CH_3$) (B) triacontanol ($CH_3(CH_2)_{29}OH$) (C) a carboxylic acid (D) 1-octadecylamine ($CH_3(CH_2)_{17}NH_2$) at the solid–liquid interface. A molecule is indicated by a white line. Reproduced with permission of the American Chemical Society (ref. 19).

Normal alkanes adapt a fully extended conformation and order in lamellae with their molecular axis parallel to the HOPG surface (like most long chain hydrocarbons) and perpendicular to the lamella axis (Fig. 1A). Moreover, the long axis of the alkanes is aligned along one of the symmetry axes of graphite, demonstrating the influence of the substrate on the two-dimensional ordering. Alcohols order in lamellae too, but they are not oriented perpendicular to the lamella axis but are tilted instead which allows for hydrogen bonding while maintaining a stable packing of the alkyl chains (Fig. 1B). Fatty acids are also typical hydrogen-bonding compounds. The carboxylic acid groups form dimers and the molecular axis is perpendicular to the lamella axis, irrespective of the length of the alkyl chain.

(Fig. 1C). Amines on the other hand are tilted, just like the alcohols and form a hydrogen-bonded network (Fig. 1D). The interactions with the underlying graphite substrate and the specific details of the hydrogen bonding drive these long alkyl chain derivatives to adopt the packing described. Other versatile compounds displaying hydrogen bonding are alkylated isophthalic acid (1,3-benzenedicarboxylic acid) and terephthalic acid (1,4-benzenedicarboxylic acid) derivatives. 5-Alkoxyisophthalic acid derivatives form close-packed arrays of interdigitating hydrogen-bonded ribbons (Fig. 2A).[20,21] In contrast to the 3D crystals, the alkyl chains and the isophthalic acid groups are confined in the same plane. As a result, the hydrogen bonding motif does not reflect the traditional dimer formation of the carboxylic acid functions but a more complex 2D hydrogen-bonding pattern is formed. By changing the location and the nature of the alkyl chains on the isophthalic acid groups, various other 2D motifs can be formed (Fig. 2B-D).

Some functionalised hydrocarbons may display stabilising hydrogen bonding along the lamella axis. For example, in monolayers of dialkylated terephthalic acid derivatives the terephthalic acid groups (bright) are linked by hydrogen bonds (the distance between the terephthalic acid groups is the same as the distance found in 3D crystals), and the alkyl chains, which are oriented perpendicular to the lamella axis, are interdigitated (Fig. 3A). In this way, infinite 1D arrays of hydrogen-bonded terephthalic acid groups are formed. Other examples of infinite 1D arrays include those formed by urea or amide derivatives.[22] The urea function provides an especially strong intermolecular interaction. As a result, it was demonstrated that 1D rows or incomplete rows could be formed and imaged at the solid–liquid interface. Those hydrogen bonded arrays and the adsorbate–substrate interactions are strong enough to immobilise the molecules on the substrate, without forming a two-dimensional network (Fig. 3B).[22]

Recent attempts describe the supramolecular ordering of trimesic acid (1,3,5-benzenetricarboxylic acid) under UHV conditions[23,24] and at the solid–liquid interface.[25] It is a polyfunctional carboxylic acid with threefold symmetry comprising a phenyl ring and three identical carboxyl end groups in the same plane (Fig. 4). Due to the trigonal exodentate functionality, the most common motif identified therein is a planar honeycomb network structure formed through the dimerisation of the carboxyl groups.[23] At low temperature on a Cu surface, it was found that trimesic acid indeed forms predominantly islands with a honeycomb lattice, however slightly distorted, which as in the case of the isophthalic acid derivatives was attributed to the adsorbate–substrate interactions. Long range order was however not achieved by this system. At room temperature (but under UHV conditions), the molecules form a stripe structure which is attributed to the fact that the molecules are not flat lying anymore but are in an upright position induced by Cu-carboxylate formation after deprotonation on the surface. Heckl *et al.* found that in addition to the honeycomb lattice, trimesic acid forms also a flowerlike motif on natural grown graphite under UHV conditions (Fig. 4).[24] The STM images were obtained at 25 K. The latter motif differs from the honeycomb lattice in the connection between the hexagons: hydrogen bonds are formed between three molecules between neighbouring rings. These authors found

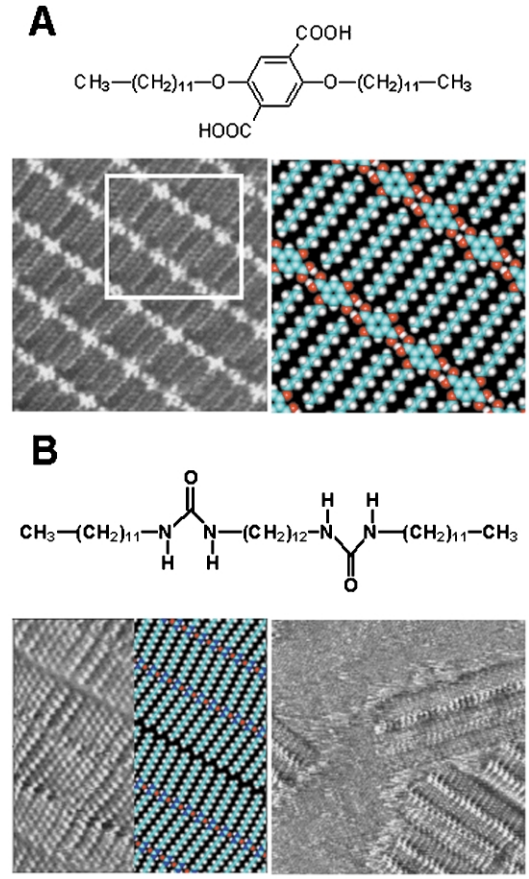

Fig. 3 STM image at the solid (HOPG)–liquid (phenyloctane) interface of (A) a terephthalic acid derivative. The bright structures are the terephthalic acid groups. The model refers to the area indicated. (B) A bis-urea derivative. Left: STM image and molecular model (7.1 nm × 7.1 nm). Right: STM image with incomplete surface coverage (17.7 nm × 17.7 nm). Adapted with permission of the American Chemical Society from refs. 21 and 22.

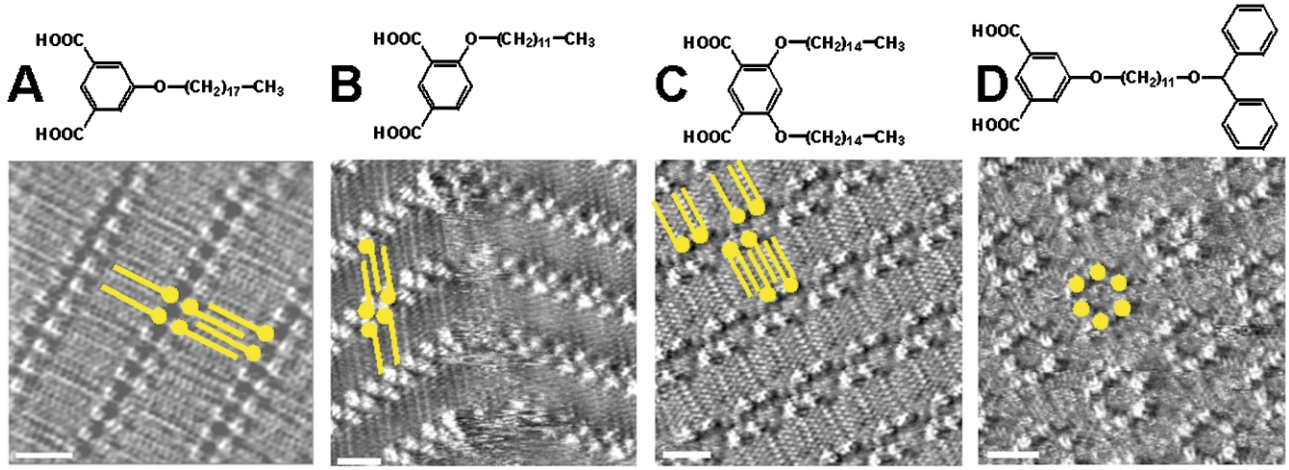

Fig. 2 STM images of isophthalic acid derivatives, illustrating the effect of number, position and nature of the alkyl chains on the 2D ordering. The 'discs' represent isophthalic acid groups. The lines are alkyl chains. In c, not all alkyl chains are adsorbed on the surface. In d, the isophthalic acid groups form a hexamer. The scale bar is 2 nm.

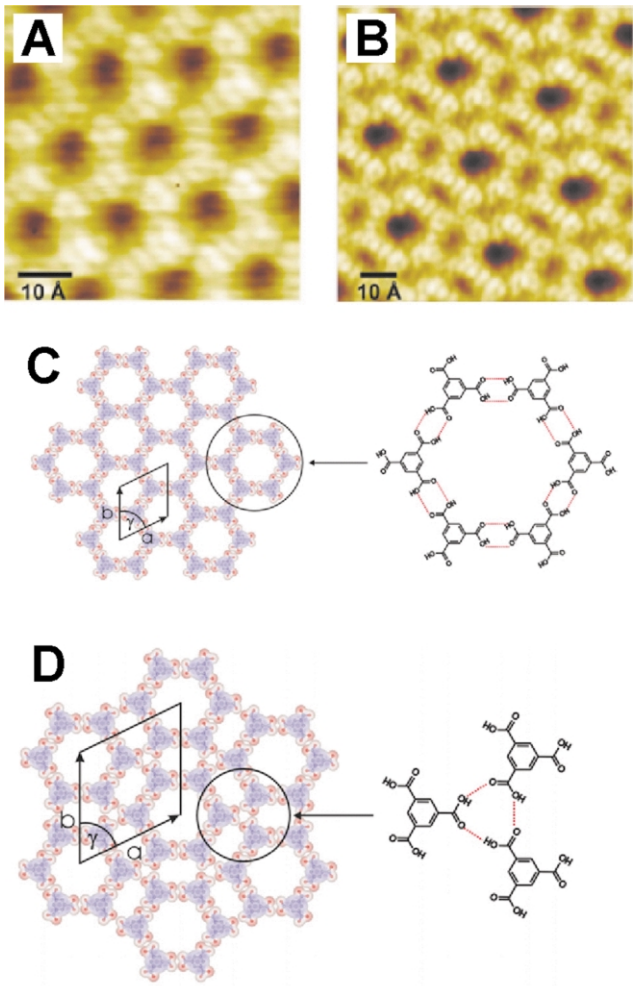

Fig. 4 (A,B) STM images of trimesic acid on graphite under UHV conditions. (A, C) honey-comb (B, D) flower structure. Adapted from ref. 24 with permission of Wiley-VCH.

that the cyclic hexamers could act as host for guest molecules, which can be stabilised by hydrogen bonding. In the honeycomb type structures, the guest molecules are lying flat within the cyclic hexamer while for the flower type structures two modes have been observed: one lying flat within the ring and the other one sitting in a top position above the ring, or standing in an upright position.

Another appealing study performed on this compound was obtained at the solid–liquid interface, under potential control.[25] By electrode potentials, one can induce self-organisation via the acceleration of molecular mobility on the surface or via promotion of the adsorption–desorption equilibrium at the Au(111)–water interface. Under no potential control, the molecules adsorb randomly on the bare surface due to the strong interaction between trimesic acid and the gold surface. Between the potentials of random adsorption and complete desorption, trimesic acid forms highly ordered adlayers. The electrode potential can regulate the interactions between adsorbates and substrates to induce self-organisation on the surface. At the more positive potentials, an extended honeycomb lattice is formed. The network structure is regulated by both the intermolecular interactions and the adsorbate–substrate interactions. This epitaxial interaction is expressed by longer than normal hydrogen bonds. At more positive potentials, a close-packed 2D network is formed.

Lei *et al.* reported on the surface stabilised porphyrin and phthalocyanine 2D network formation connected by hydrogen bonds (Fig. 5).[26] They have co-deposited a porphyrin derivative and stearic acid on HOPG. It was observed that adsorption of the porphyrin derivative alone on the surface of HOPG did not yield observable molecular images while in presence of stearic acid, 2D islands of the porphyrin derivative were absorbed, surrounded by lamellae of stearic acid. In the porphyrin domains, the molecules are arranged with 4-fold symmetry (Fig. 5). The 2D ordering is a compromise between the intermolecular interactions (hydrogen-bonding) and the minimisation of the surface free energy: in the hypothetical closest packing, no hydrogen bonding is possible; those configurations with optimal hydrogen bonding would lead to large voids; the observed packing is a compromise between both (Fig. 5C).

Based upon the self-organisation of the DNA double helix in nature, Heckl and co-workers published impressive results on the self-assembly of DNA bases at the interface between water and the surfaces of crystalline inorganic solids. The interaction between the bases is based upon hydrogen bonding. Their investigations are motivated by the possible relevance of self-assembled monolayers of DNA bases to the origin of life.[27] These authors suggest that the thermodynamically favourable formation of chiral structures through the self-assembly of achiral prebiotically available molecules onto mineral surfaces which show no asymmetry may have had some significance for the development of biomolecular homochirality in the early stages of the origin of life.[28]

Another interesting example is the supramolecular ordering of 4-[*trans*-2-(pyrid-4-vinyl)]benzoic acid (PVBA), studied by STM on noble metal surfaces under UHV conditions after deposition of the molecules by OMBE (Fig. 6).[29,30] This molecule carries a benzoic acid function and a pyridine function. The former one can act as hydrogen bond donor and acceptor while the latter functionality is a hydrogen bond acceptor. On a palladium substrate, deposition at room temperature leads to isolated molecules, which do not associate due to the strong adsorbate–substrate interactions. When small amounts of PVBA were evaporated on the close-packed surfaces of Ag at low temperature (125 K), the molecules self-assemble into networks and meandering chains are formed (Fig. 6A) while at room temperature, twin chains stabilised by

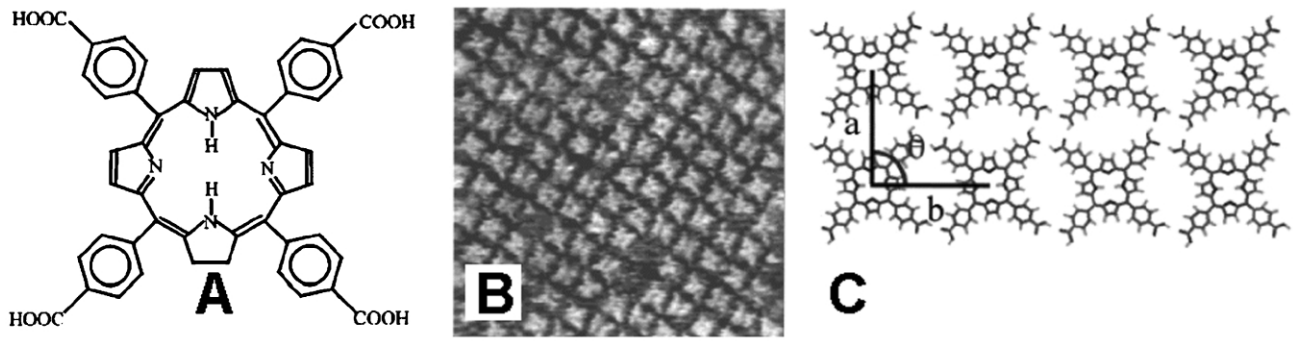

Fig. 5 (A) Chemical structure, (B) STM image (22 nm × 22 nm), and (C) molecular packing of a porphyrin derivative. Note that the hydrogen bonding between the carboxylic acid groups is not optimal, but allows a dense packing. A domain of the porphyrins is surrounded and stabilised by a monolayer of stearic acid (not shown). Adapted with permission of the American Chemical Society from ref. 26.

formation of hydrogen bonds evolve at the surface (Fig. 6B). This self-assembly of twin chains occurs at room temperature where the surface mobility of PVBA is appreciable. The twin rows are stabilised by strong head-to-tail intermolecular HO---N bonds, with the location of the corresponding OH groups at the outer side of the twin chains. A weak lateral stabilising interaction is suggested between the carbonyl group and the H-atom of the pyridine ring in an adjacent molecule. Twin chains form 'nanogratings' extending over micrometer-size domains. This is surprising given that adjacent twin rows are nanometers apart from each other and no interaction is possible between adjacent chains. The authors invoke the metastability of triple chains, which act as intermediate species in the evolution of the grating.

A comparison with (4-(pyridyl-4-yl-ethynyl)benzoic acid) (PEBA) under UHV conditions is shown in Fig. 7.[30] This molecule also contains a benzoic acid group and a pyridine function. In contrast to PVBA, PEBA organises in islands, which consist of parallel chains. The tendency to head-to-tail hydrogen bonding is apparent from the fact that the molecules at the chain ends rearrange to saturate the end groups and that the borders of the islands are almost perfectly straight.

Both molecules differ in the pattern they form: PVBA forms twin rows while PEBA forms 2D islands, which is rationalised as follows. For both molecules, the main intermolecular interaction is head-to-tail hydrogen bonding. However, different lateral interactions between molecules are responsible for the differences in the 2D patterning.

Not only on the basis of hydrogen bonding can well-defined 2D supramolecular structures be formed. Yokoyama *et al.* have discussed the self-assembly of adsorbed molecules into larger structures by controlling selective intermolecular interactions.[31] They created surface-supported supramolecular structures whose size and aggregation pattern are rationally controlled by tuning the non-covalent dipole–dipole interactions between individual adsorbed molecules. Using low temperature STM, they showed that cyano-substituted porphyrins adsorbed on a gold surface form monomers, trimers, tetramers or extended wire-like structures (Fig. 8). Porphyrins with one cyano group self-assemble into well-defined trimers. Introduction of another cyano substituent at 90 degrees leads to the formation of tetramers. If on the other hand both cyano groups are at an angle of 180 degrees, 'infinite' 1D wires (up to 100 nm long) are formed.

As a last example, Böhringer *et al.* have investigated the self-assembly of 1-nitronaphthalene (NN) on Au(111) surfaces studied with low-temperature STM.[32,33] Nitronaphthalene is of interest due to its approximately dipolar electrostatic charge distribution introduced by the NO_2 group. Interestingly, at a coverage up to 0.15 monolayer, NN decamers nucleate. All decamers exhibit a modified pinwheel structure with a core of two molecules surrounded by eight peripheral molecules. In the medium coverage range, 1D structures prevail, composed of straight or zig-zag molecular double chains within the fcc domains and at higher coverages also within the hcp domains for the straight chains. For images on pinwheel structures, see Fig. 17 in Part 5.

Several times it has been mentioned that the hydrogen bonding patterns or distances are not identical to the ones observed in 3D crystals or modelled. This is because the 2D ordering is always the result of the compromise between adsorbate–adsorbate and adsorbate–substrate interactions and the confinement to two dimensions. This has important consequences for the design of supramolecular structures on surfaces.

4 Multicomponent supramolecular structures

Given that the fabrication of highly ordered monocomponent supramolecular structures at the surface is not always trivial, the controlled formation of multicomponent composites with a well-defined ordering forms an even bigger challenge. For example, most binary mixtures investigated so far show phase separation on the nanometer scale or the formation of randomly mixed monolayers.[34] In this section, we will look in greater detail at a few examples which make use of the information at the molecular level, expressed in the ability to undergo directional non-covalent interactions, to form stoichiometric assemblies with two or more components.

In solution and in 3D crystals, such stoichiometric assemblies have been realised. The first example of such well-defined assemblies in two dimensions was carried out at the solid–liquid interface with alkylated isophthalic acid derivatives.[20] The introduction of a bifunctional aromatic base such as 2,5-dimethylpyrazine leads to strong hydrogen bonding between the COOH group and the N atom of the diazine, which, in turn, changes the self-assembly pattern (Fig. 9A). The 2D structure consists of hydrogen bonded strands of acid molecules. The alkyl side chains of two neighbouring strands interdigitate and the resulting lamellae are cross-linked by diazine molecules. These authors noted that a dimethylpyrazine leads to less dynamic and better resolved monolayer pictures compared to the methyl-free diazine. The methyl groups are visible in the STM images and lead to a higher stability due to their space-filling properties. Not only diazine molecules can co-adsorb in a well-defined pattern. For the same class of (chiral) isophthalic acid derivatives, it was observed that co-adsorption could be realised at the solid (HOPG)–liquid (1-alcohol) interface.[21] The solvent molecules are co-adsorbed at the interface between two rows of isophthalic acid groups and are stabilised by hydrogen bonding. The number of co-adsorbed solvent molecules equals the number of isophthalic acid groups (Fig. 9B). Similarly, (chiral) stearic acid derivatives and 4,4′-bipyridine form well-defined monolayers in a 2 : 1 ratio.[35] Co-adsorption provides an elegant approach to immobilise molecules on a surface which are otherwise too mobile. Similar highly organised patterns were formed for a mixture of iodooctadecane and alkyl-substituted phthalocyanines. These molecules self-assemble in

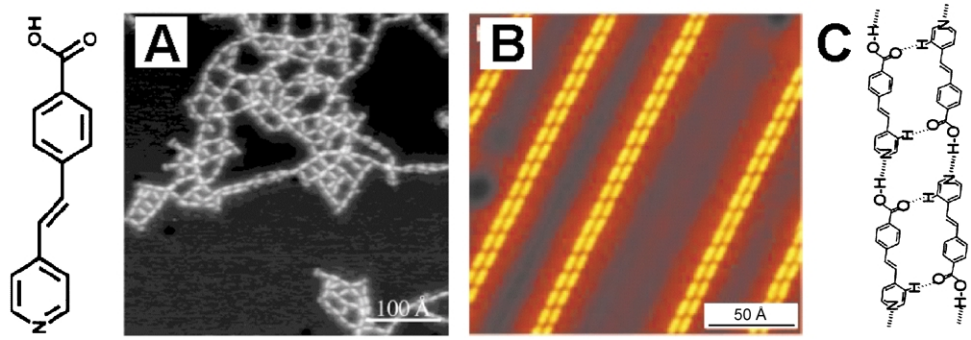

Fig. 6 (A) STM image of PVBA on Ag(111) at 125 K. (B) STM image on Ag(111) of a sample prepared at 300 K (measured at 77 K) showing the twin rows. (C) Molecular model of B. Adapted with permission of the American Chemical Society (ref. 30) and of Wiley-VCH (ref. 29).

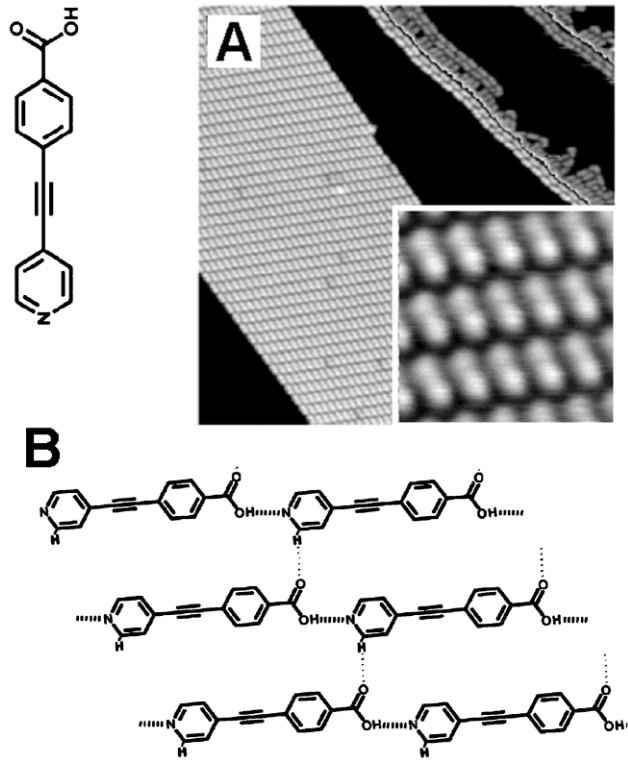

Fig. 7 (A) STM image on Ag(111) of PEBA adsorbed at 150 K and annealed at 300 K. (38 nm × 38 nm). The inset at the lower-right corner is a zoom (4.8 nm × 4.8 nm) (B) Molecular model of packing in B. Adapted with permission of the American Chemical Society (ref. 30).

alternating rows of alkanes and phthalocyanines in a 4 : 1 ratio. In spite of this highly regular arrangement, the intermolecular interactions driving this highly structured self-assembly are unknown (Fig. 9C).[36]

In addition to hydrogen bonding, other types of interaction, such as perfluorophenyl–phenyl interactions, are very well suited for self-assembly purposes. The perfluorinated cobalt phthalocyanine (F16CoPc) molecules do not form an ordered structure when deposited on Au(111).[37] This disorder and lack of submolecular resolution is in contrast to the behaviour of the protonated complex, which is attributed to differences in van der Waals attraction and electron affinities. Ni tetraphenyl porphyrin (NiTTP) forms a simple 2D crystal structure when adsorbed on gold. A 2 : 1 mixture of NiTTP and F16CoPc forms in addition to disordered regions and ordered regions of NiTPP, well-ordered regions of an entirely new structure with 1 : 1 composition as shown in Fig. 10. The phthalocyanine molecules can easily be identified by the Co ions, which appear bright.

Samori *et al.* reported on epitaxial composite layers of electron donors and acceptors of large polycyclic aromatic hydrocarbons at the solid–liquid interface (Fig. 11).[38] Hexabenzacoronene (**1**) is known as a strong electron donor while the alkylated coronenebis(dicarboximide) derivative (**3**) is a potent electron acceptor. Films prepared by co-deposition exhibit an oblique arrangement. Interestingly, on top of a layer of donor molecules, within the same layer between two physisorbed donor molecules, acceptor molecules are co-adsorbed in a well-defined arrangement. Moreover, under pure donor sample preparation conditions, a stable second layer of donor molecules could never be achieved. On the other hand, when the acceptor co-crystallises, the second layer is stabilised.

The last example differs from all the previous systems discussed because it does not form very regular stoichiometric composites. However, it illustrates a procedure that leads to the formation of linearly arranged ligand-stabilised Au_{55} clusters. This approach utilises the incorporation of chemically modified Au_{55} nanoclusters into highly oriented molecular templates by

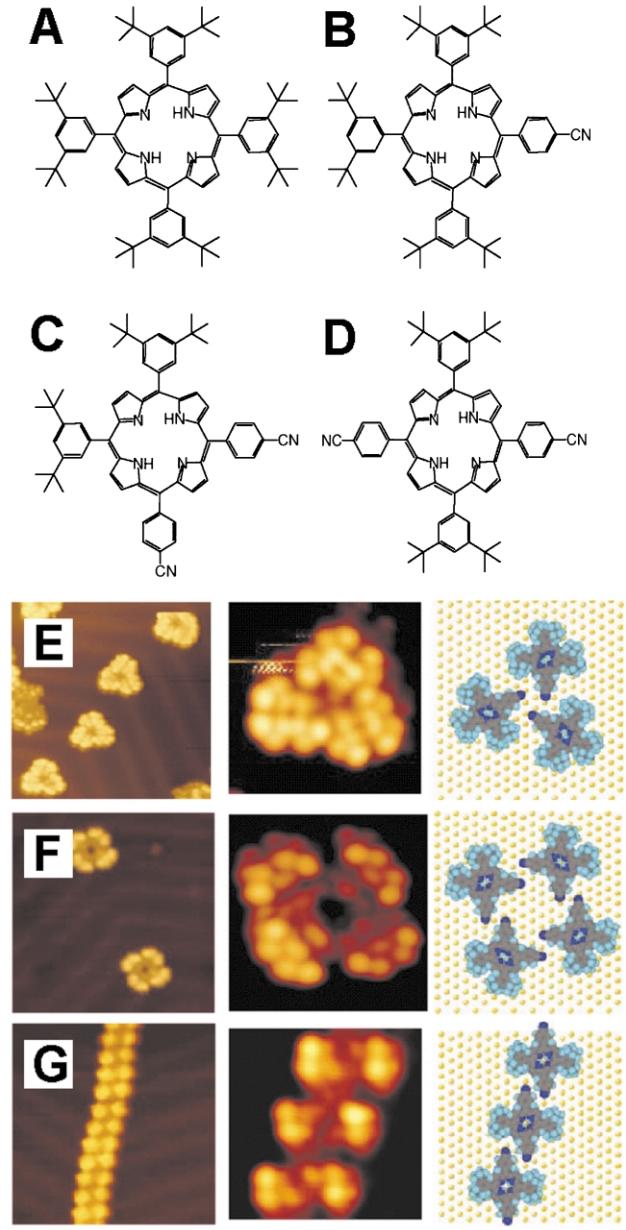

Fig. 8 STM image at 63 K of supramolecular aggregations induced by the cyano groups on Au(111). (A–D) Chemical structures. (E–G) respective STM images of structures B, C and D. Reprinted by permission from Nature (ref. 31) copyright 2001 Macmillan Publishers Ltd.

substitution of individual molecules of the template at the solid–liquid interface. The molecular templates guide the incorporation of Au_{55} clusters resulting in strands of linearly arranged nano-objects and represent self-organised nano-structures with a periodicity down to a few nanometers (Fig. 12).[39]

5 Two-dimensional chirality

Since the late nineties, the expression of molecular chirality at surfaces has received increasing attention. STM provides an especially convenient approach to investigate (sub)monolayers, and the chirality aspects thereof, with submolecular resolution. It is one of the very few techniques that allow identifying the (sub)monolayer chirality and even absolute conformation. It is not the purpose of this review to give an extensive overview of all the work that has been reported on chirality at surfaces but this section is intended to give a flavour of the relation between self-assembly directed non-covalent interactions and chirality at surfaces.[40] Chiral discrimination between mirror image stereoisomers can lead to the spontaneous spatial separation of a

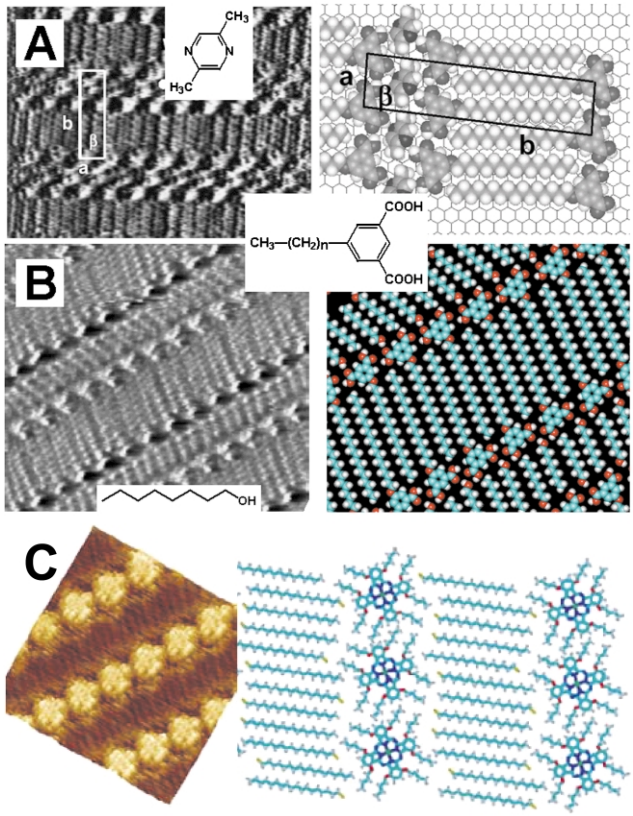

Fig. 9 (A) Left: STM image (10.0 nm × 8.8 nm) of a 2:1 mixture of a 5-alkoxyisophthalic acid derivative and 2,5-dimethylpyrazine (insert) at the solid–liquid interface. Right: Molecular model. (B) Left: STM image (12.9 nm × 9.7 nm) of a 1:1 mixture of a 5-alkoxyisophthalic acid derivative and 1-octanol (inset) at the solid–liquid interface. Right: Molecular model. (C) Left: STM image (12 nm × 12 nm) of a 1:4 mixture of an alkyl-substituted phthalocyanine with 1-iodooctadecane at the solid–liquid interface. Adapted with permission of Wiley-VCH from ref. 20, reprinted with permission from the American Chemical Society from ref. 21 and ref. 36.

racemic mixture into the enantiomerically pure phases. In 3D systems the formation of these so-called conglomerates is rather the exception than the rule: most racemic mixtures crystallise as racemates with the unit cell composed of an equal number of molecules with opposite handedness or as random solid solutions. Due to the confinement of the molecules in a plane

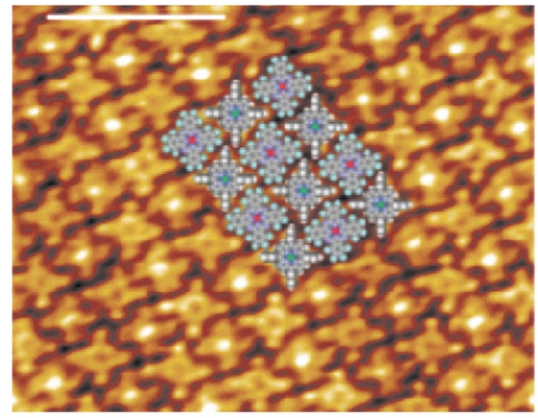

Fig. 10 STM image of 1:1 mixed monolayer of NiTPP and F16CoPc. The F16CoPc molecules can easily be recognised by the bright Co atoms. The scale bar is 5 nm. Adapted with permission of the American Chemical Society from ref. 37.

and the interaction with the substrate, conglomerate formation becomes more likely.

5.1. Enantiopure molecules

Mirror image molecules always form mirror image supramolecular structures on a surface. Kühnle *et al.* reported on the chiral recognition in dimerisation of adsorbed cysteine, a natural amino acid.[41] Pure cysteine enantiomers adsorb as pairs on the gold surface. Pairs of D-cysteine are the mirror image of pairs of L-cysteine with respect to the symmetry of the gold surface. The molecules are chemisorbed on the gold surface, the carboxylic acids form hydrogen bonds. In addition, when depositing a racemic mixture of cysteine onto the gold surface, molecular dimers identical to those formed by the enantiopure cysteine molecules are observed. The chiral recognition in this bimolecular system can be explained by a three-point contact model (Fig. 13A). Raval *et al.* reported on the extended surface chirality from supramolecular assemblies of adsorbed chiral molecules, which are of relevance to heterogeneous enantioselective catalysis.[42] The STM images reveal that the (*R*,*R*)-bitartrate molecules are self-assembled in rows of three, each row stacking in parallel with others to from long chains. The growing direction does not coincide with one of the symmetry

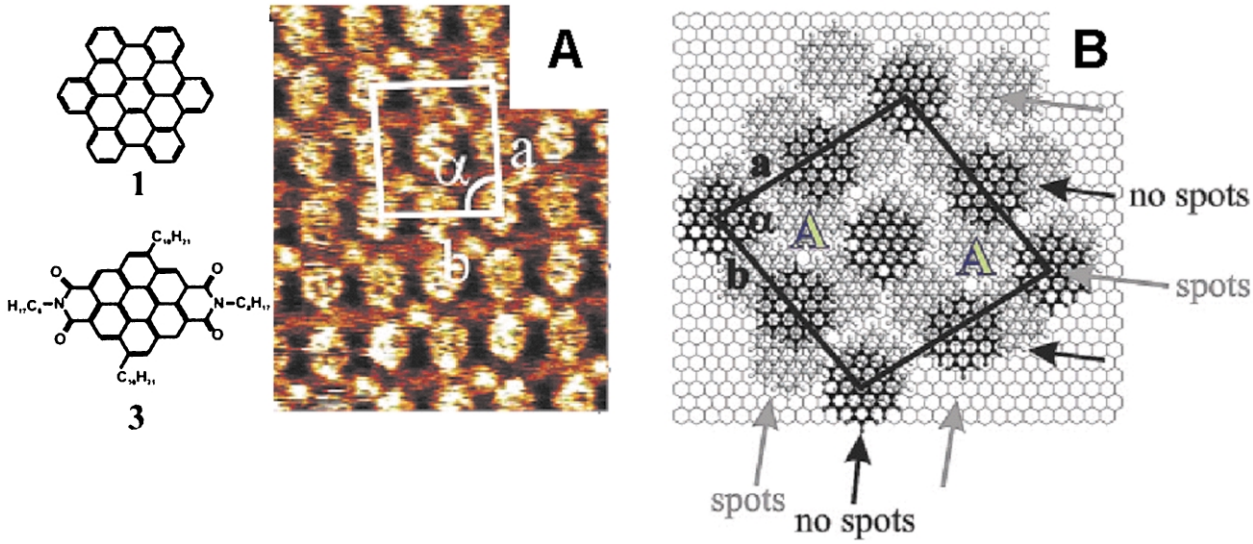

Fig. 11 (A) STM image at the solid (HOPG)–liquid interface of a mixture of **1** and **3** (image size is 11 nm × 13 nm). It is an image of a second epitaxial layer with a donor–acceptor stoichiometry of 2:1 on top of a first epitaxial layer of 1. The large features are **1**, the smaller and brighter features are **3**. Compound **3** packs only every second row probably because of its preferential adsorption on the electron donor disk of **1**, which is exposed in the underlying first $C_{42}H_{18}$ layer. Adapted with permission of the American Chemical Society of ref. 38.

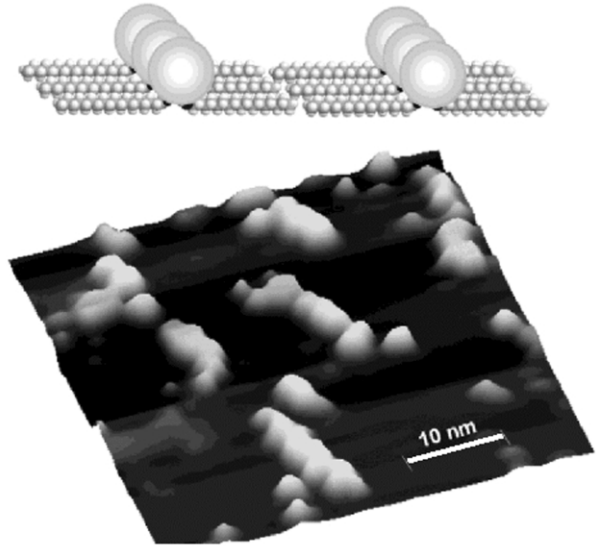

Fig. 12 STM image of Au_{55} nanoclusters co-adsorbed between $C_{14}H_{29}COOH$ rows at the solid (HOPG)–liquid interface. The ordering of the gold nanoclusters (bright features) is correlated with the periodicity of the lamella fatty acid template structure. Adapted with permission of the American Chemical Society from ref. 39.

directions of the underlying metal surface, which implies the creation of a chiral surface that is non-superimposable on its mirror image. This self-assembly was attributed to the close proximity of the hydroxy groups on neighbouring bitartrate molecules, leading to intermolecular hydrogen-bonding interactions that extend across the surface. *R,R*-tartaric acid and *S,S*-tartaric acid form identical 2D patterns. However, the respective patterns are related by mirror symmetry. The mirror positions of the OH groups in the two enantiomers lead to a switch in supramolecular assembly directions (Fig. 13B). Other examples involving hydrogen bond formation include terephthalic acid derivatives (Fig. 14)[43] with chiral side chains (*R,R*) or (*S,S*) at the solid–liquid interface or carboxylic acid derivatives where the *R* and *S* enantiomer form enantiomorphous monolayers.[44] In most cases, the reason why enantiomorphous 2D structures are formed from enantiopure compounds is simple: 1) most compounds organise into oblique unit cells, which by definition are 2D chiral. 2) The supramolecular structures formed by enantiopure compounds will have the same energy only if their structures are related by mirror symmetry due to stereospecific interactions. These relations hold also for the self-assembly of multi-component systems, *e.g.* isophthalic acid–1-octanol[45] and chiral stearic acid derivative–4,4′-bipyridine,[35] introduced in Part 4. Interestingly, the relative orientation of the achiral molecules expresses the chirality of the domains in which they are co-adsorbed.

5.2. Racemic mixtures

The question whether a racemic mixture of chiral molecules undergoes spontaneous separation into enantiopure domains is of special interest. Will a racemate form or will the molecules undergo spontaneous spatial resolution? In most cases spontaneous resolution will occur. A racemic mixture of cysteines forms D,D and L,L pairs (Fig. 13) and also for 2D monolayers, all experimental evidence hints at spontaneous resolution. Important to note is that most achiral molecules become 2D chiral upon adsorption on a substrate. Consider for instance PVBA: this molecule can be placed in two different ways on a surface: they cannot be superimposed by any in plane translation or rotation and are 2D chiral.[46] Therefore, applying achiral molecules on a substrate is like depositing a racemic mixture. Fig. 15 shows that the constituent molecular rows of the twin

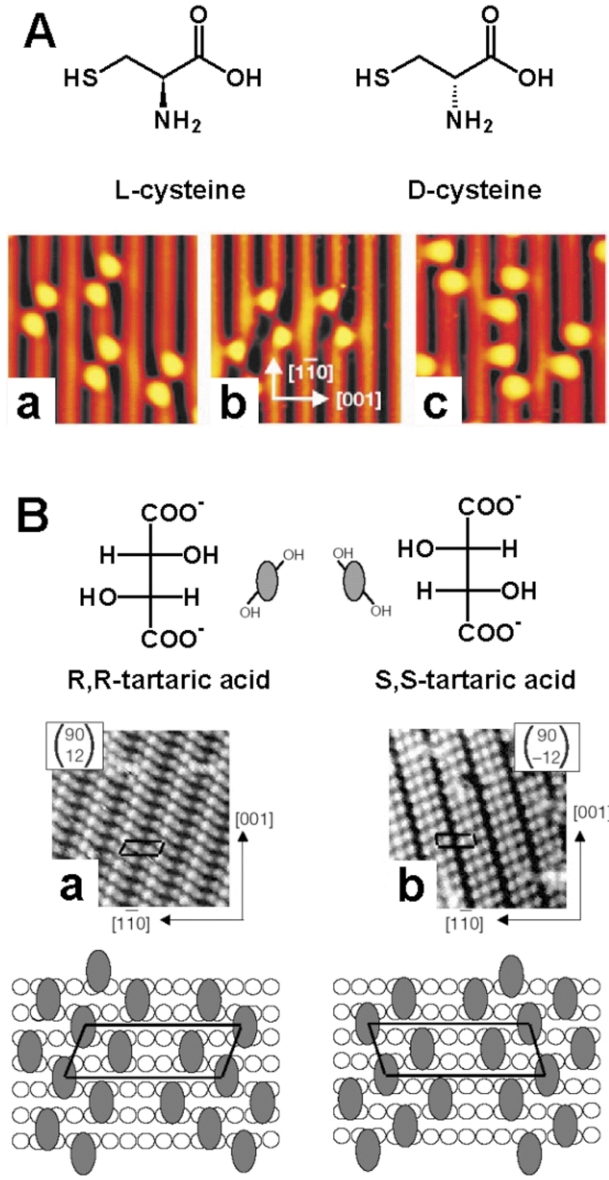

Fig. 13 (A) STM images on Au(110) surface of (a) L-cysteine pairs (b) D-cysteine pairs (c) Molecular pairs formed from DL-cysteine. Image size is 49 Å × 53 Å. (B) STM images on Cu(110) of (a) *R,R*-tartaric acid monolayers and (b) *S,S*-tartaric acid monolayers. The image size is 108 Å × 108 Å. Reprinted by permission from Nature (ref. 41 and ref. 42) copyright 2001 and 2000 Macmillan Publishers Ltd.

chains can have two relative displacements, related by a mirror symmetry. Therefore, the twin chains display supramolecular chirality. Molecular dynamics simulations indicate that all the molecules in a twin chain have the same 2D chirality suggesting real spontaneous chiral resolution. It is deduced that self-replication of supramolecular chirality takes place in the course of the gratings' evolution.

An interesting case is provided by comparison with the supramolecular patterns (islands) formed by PEBA.[30] Although the molecule is 2D achiral, the islands represent a pair of enantiomorphic supramolecular structures because of a distinct shift of adjacent molecular chains in the islands and consequently are not simply rotational domains (Fig. 16). In contrast to PVBA where 2D-enantiomers assemble in supramolecular chiral structures because of resolution of a racemic mixture, in the PEBA case, enantiomorphic structures result from the distinct packing of an achiral species.

The formation of supramolecular clusters by nitronaphthalene (NN) forms another interesting case.[32,33] STM images of the NN covered Au(111) surface at about 70 K reveal that molecular aggregates of distinct size and geometry have self-assembled. These authors found that about 85% of these

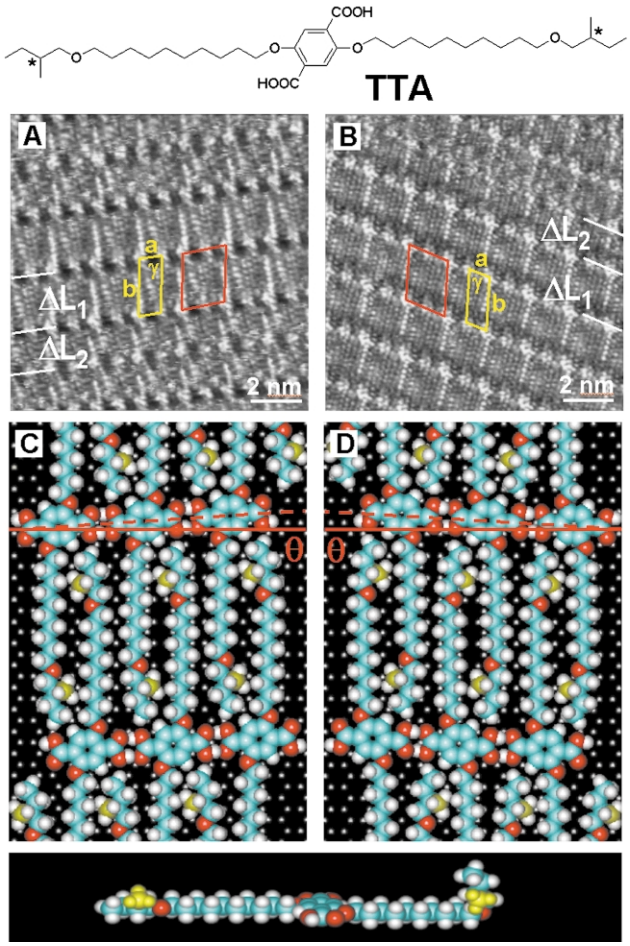

Fig. 14 STM images at the solid (HOPG)–liquid interface and model of (A,C) *R*,*R*-TTA and (B,D) *S*,*S*-TTA. Both enantiomers form mirror image type patterns. Bottom: alkyl chains are not always extended: the 2-methylbutoxy group is often raised up from the HOPG surface (ΔL_2). The monolayer unit cell (for the fully extended alkyl chains (ΔL_1)) is indicated in yellow. The red unit cell refers to the epitaxy with the HOPG surface. Adapted with permission of the American Chemical Society from ref. 43.

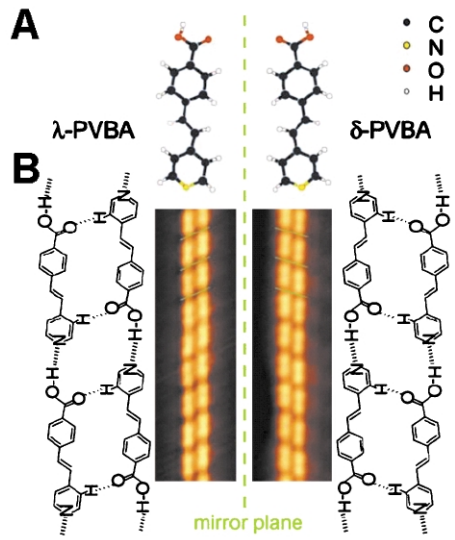

Fig. 15 (A) Mirror image relationship between the two possible adsorption geometries of PVBA. (B) Models and STM images of the chiral twin chains. Adapted with permission of the American Physical Society from ref. 46.

structures are composed of ten molecules arranged in a modified pinwheel structure (Fig. 17). Two related kinds of decamers are observed, which behave in a similar manner to an

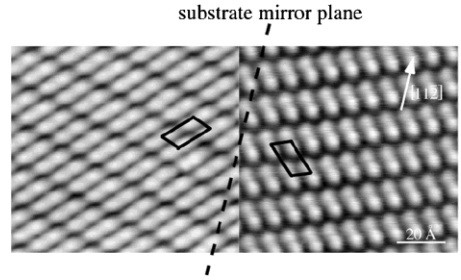

Fig. 16 Enatiomorphism of PEBA islands on Ag(111). Two mirror domains together with their respective unit cells are shown. Printed with permission of the American Chemical Society from ref. 30.

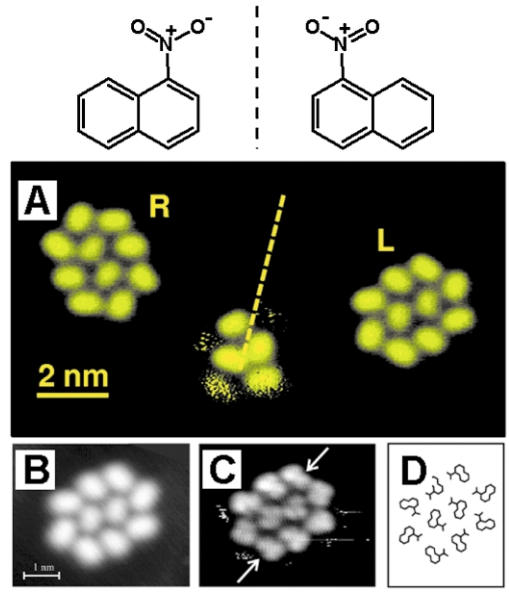

Fig. 17 Mirror image relationship between the two possible adsorption geometries of NN. (A) Two-dimensional chiral decamers (denoted L and R) formed by NN molecules on the Au(111) surface. The dashed line is the mirror plane. (B, C). High-resolution images of a decamer and (D) a molecular model obtained by molecular dynamics simulations. Decamers are comprised of an even number of l and r molecules in a 8 : 2 ratio (or vice versa). Adapted with permission from Wiley-VCH (ref. 33) and the American Physical Society (ref. 32).

object and its mirror image and cannot be transformed into one another by rotation and translation with the surface plane. Note that the mirror symmetry does not mean that a decamer consists exclusively of l or r molecules, as one might think: however, the inversion of symmetry implies that they are composed of an even number of l and r molecules. Molecular dynamics calculations performed by these authors suggest a 8 : 2 ratio (2 : 8 for the opposite chirality). Moreover, these authors demonstrated in a most elegant way the manipulation capabilities of STM. By adjusting the experimental tunneling parameters, they achieved in laterally moving clusters over the surface, without affecting the chirality and the supramolecular arrangement of the clusters. These experiments indicate that the decamers behave as supermolecules whose stability, structure, and chirality are determined by intermolecular interactions. They achieved separating R and L clusters in separate domains on the surface. This '2D' experiment is similar to the famous experiment performed more than 150 years ago by Pasteur. In analogy with tweezers and a magnifier which Pasteur needed to mechanically resolve enantiomorphic crystals obtained form a solution of racemic sodium ammonium tartrate, these authors used the STM tip to identify the enantiomorphous clusters and to separate them.

6 Dynamics

As mentioned before, mobility is important. On the one hand, the mobility of the molecules has to be restricted to allow successful STM imaging. On the other hand, mobility is necessary for the formation of supramolecular structures. Under UHV conditions, the mobility can be influenced and controlled by the monolayer coverage and temperature control and the diffusion or rotation of molecules can be studied.[47,48] An example is given in Fig. 18 which involves a 2D solid–gas

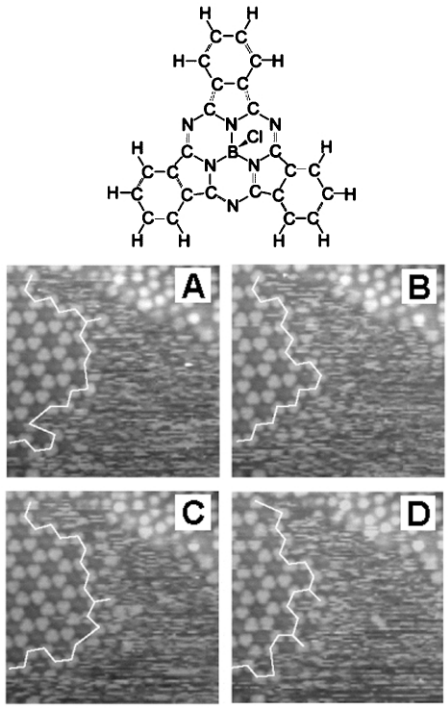

Fig. 18 Chemical structure of SubPc and a sequence of STM images showing the time evolution of a condensed molecular island. The interval time between two images is 3 min 26 s. Scan range is 25.8 nm × 25.8 nm. The SubPc molecules appear bright in the images. The white line connects the outermost molecules. Printed with permission of Elsevier from ref. 48.

equilibrium. Sub-phthalocyanine (SubPc) molecules self-assemble in a 2D crystalline overlayer with a honeycomb pattern characterised by a low packing density (2D-condensed phase). Next to a condensed island, noisy streaks appear in the scan direction, indicating that they exhibit mobility on the time scale of one scan line (2D-gas phase). These domains evolve in time as shown by time-lapse imaging sequences. The borders of the 2D-condensed phase move as a function of time, indicating that the condensed phase is in dynamic coexistence with the gas phase. These two phases coexist in a 2D thermodynamic equilibrium at room temperature.

In addition to the processes which can happen on the substrate like rotational[48] and translational diffusion, and cooperative molecular motions which are involved in Ostwald-ripening (growing of larger domains at the expense of smaller domains),[49,50] at the solid–liquid interface the adlayer is in equilibrium with the supernatant solution and several examples show that there is exchange of molecules. These exchange processes are important for the formation of supramolecular structures: first, the exchange of molecules in two dimensions and in three dimensions (monolayer–supernatant solution) provides a ′healing′ mechanism to repair defects. Second, at the solid–liquid interface, the determination of the residence times of individual molecules in supramolecular networks indicates the stability of the systems in terms of adsorbate–adsorbate and adsorbate–substrate interactions.[51,52]

For instance, exchange of molecules with the supernatant solution gives rise to unique dynamics. For 5-alkoxyisophthalic acid derivatives the co-deposition process of 1-octanol molecules at the solid (HOPG)–liquid (1-octanol) interface could be followed (Fig. 19A–C). This image sequence visualises the

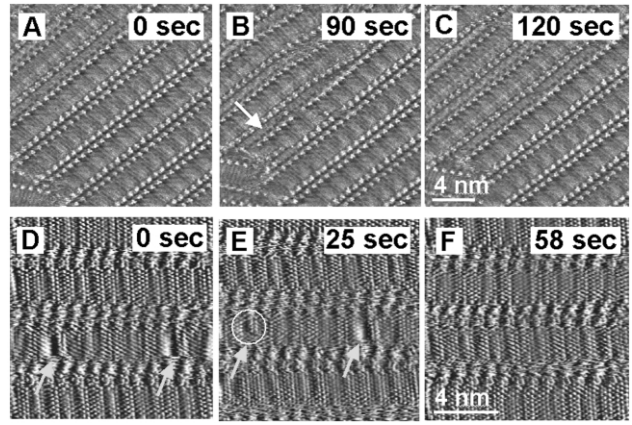

Fig. 19 (A–C) Time sequence of co-deposition of 1-octanol molecules between rows of 5-alkoxyisophthalic acid molecules at the solid (HOPG)–liquid (1-octanol) interface. The arrow in B indicates the location where the dynamic co-adsorption of 1-octanol molecules starts. (D–F). Desorption of semifluorinated 5-alkoxyisophthalic acid molecules (arrows) within a monolayer of non-fluorinated analogues. Adapted with permission of the American Chemical Society from ref. 21

insertion of 1-octanol molecules between two isophthalic acid lamellae. A domain boundary at the left (arrow) is used as a reference point. The insertion process is completed within two minutes and involves the adsorption of ~48 1-octanol molecules. Co-deposition involves the exchange of molecules with the supernatant solution and reorientation (translation) of large monolayer parts in a co-operative fashion. A direct proof for the exchange of individual molecules within a monolayer with those in the supernatant solution is shown in Fig. 19D–F. For mixed solutions of semifluorinated and non-fluorinated isophthalic acid derivatives, it was observed that if there is no difference in chain length or if the length differs only by one methylene group, mixed monolayers are formed and individual semi-fluorinated molecules are dispersed in a matrix formed by the non-fluorinated ones. The semi-fluorinated molecules can easily be identified due to the specific dark contrast (low tunneling current) of the fluorinated moiety. It was observed that semi-fluorinated molecules desorb and are replaced by non-fluorinated ones.[51] The residence time of single fluorinated molecules is on the order of seconds to several minutes, much longer than the estimated residence time reported for mixtures of saturated/unsaturated acids and alcohol/thiol mixtures by Stevens *et al.*[52] When neglecting solvent effects, this can partially be accounted for by the stabilising effect of isophthalic acid hydrogen bonding on the supramolecular network.

7 Reactivity

The possibility of carrying out reactions on adsorbed molecules is of great interest. These reactions can be induced by external stimuli such as light[53,54] or, even more appealing, by the use of the STM probe itself. Beautiful examples exist where the STM tip is used on a single molecule level to break bonds selectively, to manipulate molecular fragments or atoms, and to selectively form bonds.[55] A very exciting possibility is to produce a tailor-made supramolecular pattern, induced by careful molecular design, which leads to an optimal relative orientation of reactive groups for intermolecular reactions to occur, which would otherwise not take place if the molecules were not preorganised.

The polymerisation of diacetylenes, which is a so-called topochemical reaction, is such an example (Fig. 20A). This type

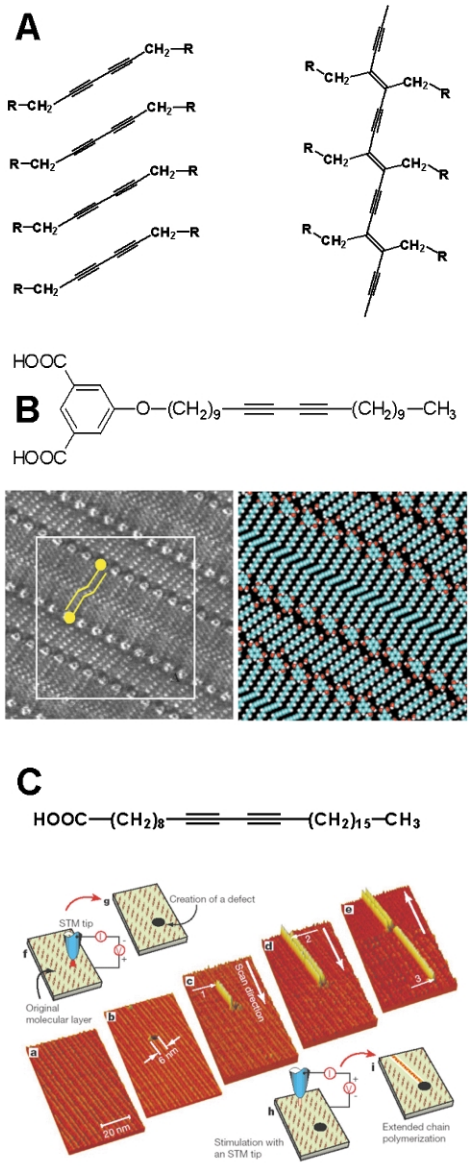

Fig. 20 (A) Left: array of diacetylene molecules. Right: polydiacetylene chain. (B) Top: Chemical structure of a diacetylene containing isophthalic acid derivative. Left: High-resolution STM image at the solid (HOPG)–liquid interface of the diacetylene derivative. The 1-undecanol solvent molecules are co-adsorbed. Two molecules are indicated by a stick model. The orientation of the diacetylene groups is easily observable. Right: Molecular model of the area indicated in B. (C) STM images and diagrams showing the process of controlling the initiation and termination of linear chain polymerisation with an STM tip. STM images are obtained at the solid (HOPG)–air interface. a) original monolayer of 10,12-nonacosadiynoic acid. b) Creation of an artificial defect. c) First chain polymerisation, initiated at the arrow. d) Second chain polymerisation, initiated at arrow. e) Third chain polymerisation, initiated at arrow. Reprinted by permission from Nature (ref. 56) copyright 2001 Macmillan Publishers Ltd.

of reaction has been extensively studied in 3D crystals and it is known that the relative orientation (angle) and distance between adjacent diacetylene monomer units is critical for the reaction to occur. Grim *et al.* demonstrated a few years ago that the polymerisation reaction could be induced at the solid (HOPG)–liquid interface by light for monolayers of a diacetylene containing isophthalic acid derivative.[54] The supramolecular ordering of the molecules, which is analogous to the 2D architecture formed by other 5-alkoxyisophthalic acid derivatives, brings the diacetylene functions close to each other with the desired orientation (Fig. 20B). The diacetylene moieties appear as bright spots in the middle of the lamellae. After in-situ illumination (254 nm) of the monolayer film on graphite, again monolayer structures are observed with an increase in distance between the isophthalic acid groups and a change in contrast of the polydiacetylene part. Recently, Aono *et al.* have reported the formation of conjugated polymer 1D structures (polydiacetylenes) by initiating the chain polymerisation of diacetylene containing carboxylic acid derivatives using a STM tip with a spatial precision on the order of 1 nm at the solid (HOPG)–air interface (Fig. 20C).[56] The molecules are aligned to form straight chains and the chains are arranged in a manner such that the COOH end groups of a chain are opposite those of a neighbouring chain. The controlled fabrication of nanowires is of importance in the field of nanotechnology. In analogy with light excitation, the STM tip initiates the reaction by applying a pulsed sample bias. A very bright line appeared, starting from the point of stimulation, which indicates that the reaction initiated by the STM tip has propagated and a polydiacetylene chain is formed. The length of the polydiacetylene chain is determined by the size of the domains of diacetylene monomer molecules having the same orientation. The initiation by the STM tip leads to polymerisation in both directions. Interestingly, these authors were able to control the length of the polydiacetylene chains within a domain. In order to achieve that, they created an artificial defect in the form of a 6 nm wide hole at a predetermined position within the monolayer using an STM tip. Such a defect terminates the polymerisation reaction. Molecular modelling shows that the polymer backbone is raised from the graphite substrate and suggests that organic molecules with various novel conformations could be created on 2D solid surfaces.

8 Conclusions and outlook

Gaining a better understanding on how molecules self-assemble on surfaces is definitely of importance given the demands of ′nanotechnology′ on surfaces. In order to make well-structured monomolecular thin films, non-covalent directional interactions are well-suited to achieve these goals. However, knowledge obtained from the self-assembly in 3D crystals and in solution can not automatically be transferred to two dimensions. In addition to intermolecular interactions, adsorbate–substrate interactions play an important role in the 2D pattern formation: the surface, in combination with the temperature, determines the strength of the interaction of the adsorbate with the surface. As a result, in a number of systems studied, it was observed that for example unexpected hydrogen bond patterns were formed or that the hydrogen bonds where longer or did not show the optimal geometry. This asks for a careful design of the molecules and the choice of the proper substrate.

Although this review mainly deals with hydrogen bonding, supramolecular architectures based upon metal complexation will become more important.[57,58,59] Metal complexation allows the formation of more rigid architectures and because of the different complexation modes, this kind of interaction can be used for the formation of templates, which are the basis for extension into the third dimension.

9 Acknowledgements

The authors thank the DWTC, through IUAP-V-03. SDF is a postdoctoral fellow of the Fund for Scientific Research-Flanders. The authors wish to express their gratitude to their long term collaborators: Prof. Müllen (Mainz), Prof. Feringa and Dr van Esch (Groningen), and Prof. Veciana and Dr David Amabilino (Barcelona), and the past and present co-workers: Dr

Peter Vanoppen, Dr Kees Grim, Dr André Gesquière, and Dr Mohamed Abdel-Mottaleb. The authors would also like to thank their colleagues for supplying original graphical material.

10 References

1 J. M. Lehn, *Supramolecular Chemistry: Concept and Perspectives*, VCH, Weinheim, 1995.
2 G. M. Whitesides, J. P. Mathias and C. T. Seto, *Science*, 1991, **254**, 1312.
3 M. C. Etter, *Acc. Chem. Res.*, 1990, **23**, 120.
4 A. Ulman, *Chem. Rev.*, 1996, **96**, 1533; and references therein.
5 P. A. Lewis, Z. J. Donhauser, B. A. Mantooth, R. K. Smith, L. A. Bumm, K. F. Kelly and P. S. Weiss, *Nanotechnology*, 2001, **12**, 231–237; and references therein.
6 G. Binnig, H. Roher, C. Gerber and E. Weibel, *Phys. Rev. Lett.*, 1982, **49**, 57.
7 H. Ohtani, R. J. Wilson, S. Chiang and C. M. Mate, *Phys. Rev. Lett.*, 1988, **60**, 2398.
8 S. R. Forrest, *Chem. Rev.*, 1997, **97**, 1793.
9 J. S. Foster and J. E. Frommer, *Nature*, 1988, **333**, 542.
10 G. C. McGonigal, R. H. Bernhardt and D. J. Thomson, *Appl. Phys. Lett.*, 1990, **57**, 28–30.
11 J. Rabe and S. Buchholz, *Science*, 1991, **253**, 424.
12 N. J. Tao, *Phys. Rev. Lett.*, 1996, **76**, 4066.
13 P. Wu, Q. Zeng, S. Xu, C. Wang, S. Yin and C.-L. Bai, *Chem. Phys. Chem.*, 2001, **12**, 750.
14 R. Kuroda, E. Kishi, A. Yamano, K. Hatanaka, H. Matsuda, K. Eguchi and T. Nakagiri, *J. Vac. Sci. Technol. B.*, 1991, **9**, 1180.
15 G. Zhang, Y. Kuwahara, J. Wu, M. Akai-Kasaya, A. Saito and M. Aono, *Surf. Sci.*, 2001, **476**, 254.
16 B. Wu, S. X. Yin, C. Wang, X. H. Qui and C. L. Bai, *J. Phys. Chem. B*, 2000, **104**, 10502.
17 S. Subramanian and M. J. Zaworotko, *Coord. Chem. Rev.*, 1994, **137**, 357.
18 S. Buchholz and J. P. Rabe, *Angew. Chem. Int. Ed. Engl.*, 1992, **31**, 189.
19 D. M. Cyr, B. Venkataraman and G. W. Flynn, *Chem. Mater.*, 1996, **8**, 1600.
20 K. Eichhorst-Gerner, A. Stabel, G. Moessner, D. Declerq, S. Valiyaveettil, V. Enkelmann, K. Müllen and J. P. Rabe, *Angew. Chem., Int. Ed. Engl.*, 1996, **35**, 1492.
21 S. De Feyter, A. Gesquière, M. M. Abdel-Mottaleb, P. C. M. Grim, F. C. De Schryver, C. Meiners, M. Sieffert, S. Valiyaveettil and K. Müllen, *Acc. Chem. Res.*, 2000, **33**, 520.
22 S. De Feyter, K. Grim, J. van Esch, R. M. Kellogg, B. L. Feringa and F. C. De Schryver, *J. Phys. Chem. B*, 1998, **102**, 8981.
23 N. Dmitriev, N. Lin, J. Weckesser, J. V. Barth and K. Kern, *J. Phys. Chem. B*, 2002, **106**, 6907.
24 S. Griessl, M. Lackinger, M. Edelwirth, M. Hietschold and W. M. Heckl, *Single Mol.*, 2002, **3**, 25.
25 Y. Ishikawa, A. Ohira, M. Sakata, C. Hirayama and M. Kunitake, *Chem. Commun.*, 2002, 2652.
26 S. B. Lei, C. Wang, S. X. Yin, H. N. Wang, F. Wi, H. W. Liu, B. Xu, L. J. Wan and C. L. Bai, *J. Phys. Chem. B.*, 2001, **105**, 10838.
27 W. M. Heckl, *Astrobiology: The Quest of the Conditions of Life*, eds. Gerda Horneck and Christa Baumstarck-Khan, Springer, 2002, p. 361.
28 S. J. Sowerby, W. M. Heckl and G. B. Petersen, *J. Mol. Evol.*, 1996, **43**, 419.
29 J. V. Barth, J. Weckesser, C. Cai, P. Günter, L. Bürgi, O. Jeandupeux and K. Kern, *Angew. Chem. Int. Ed.*, 2000, **39**, 1230.
30 J. V. Barth, J. Weckesser, G. Trimarchi, M. Vladimirova, A. De Vita, C. Cai, H. Brune, P. Günter and K. Kern, *J. Am. Chem. Soc.*, 2002, **124**, 7991.
31 T. Yokoyama, S. Yokoyama, Y. Okuno and S. Mashiko, *Nature*, 2001, **413**, 619.
32 M. Böhringer, K. Morgenstern, W.-D. Schneider, R. Berndt, F. Mauri, A. De Vita and R. Car, *Phys. Rev. Lett.*, 1999, **83**, 324.
33 M. Böhringer, K. Morgenstern, W.-D. Schneider and R. Berndt, *Angew. Chem. Int. Ed.*, 1999, **38**, 821.
34 S. De Feyter, M. Larsson, N Schuurmans, B Verkuijl, G. Zoriniants, A Gesquière, M. M. Abdel-Nottaleb, J. van Esch, B. L. Feringa, J. van Stam and F. C. De Schryver, *Chem. Eur. J.*, 2003, **9**, 1198, and references therein.
35 P. Qian, H. Nanjo, T. Yokoyama, T. M. Suzuki, K. Akasaka and H. Orhui, *Chem. Commun.*, 2000, 2021.
36 S. B. Lei, S. X. Yin, C. Wang, L. J. Wan and C. L. Bai, *Chem. Mater.*, 2002, **14**, 2837.
37 K. W. Hipps, L. Scudiero, D. E. Barlow and M. P. Cooke, *J. Am. Chem. Soc.*, 2002, **124**, 2126.
38 P. Samori, N. Severin, C. D. Simpson, K. Müllen and J. P. Rabe, *J. Am. Chem. Soc.*, 2002, **124**, 9457.
39 S. Hoeppener, L. Chi and H. Fuchs, *Nanoletters*, 2002, **2**, 459.
40 For a recent review on 'Spontaneous resolution under supramolecular control': L. Pérez-Garcia and D. B. Amabilino, *Chem. Soc. Rev.*, 2002, **31**, 342.
41 A. Kühnle, T. R. Lindertoh, B. Hammer and F. Besenbacher, *Nature*, 2001, **415**, 891.
42 M. O. Lorenzo, C. J. Baddeley, C. Muryn and R. Raval, *Nature*, 2000, **404**, 376.
43 S. De Feyter, A. Gesquière, C. Meiners, M. Sieffert, K. Müllen and F. C. De Schryver, *Langmuir*, 1999, **15**, 2817.
44 D. G. Yablon, J. S. Guo, D. Knapp, H. B. Fang and G. W. Flynn, *J. Phys. Chem. B*, 2001, **105**, 4313; and references therein.
45 S. De Feyter, P. C. M. Grim, M. Rücker, P. Vanoppen, C. Meiners, M. Sieffert, S. Valiyaveettil, K. Müllen and F. C. De Schryver, *Angew. Chem. Int. Ed.*, 1998, **37**, 1223.
46 J. Weckesser, A. De Vita, J. V. Barth, C. Cai and K. Kern, *Phys. Rev. Lett.*, 2001, **87**, 96101.
47 J. V. Barth, T. Zambelli, J. Wintterlin, R. Schuster and G. Ertl, *Phys. Rev. B*, 1997, **55**, 12902.
48 J. K. Gimzewski, C. Joachim, R. R. Schlittler, V. Langlais, H. Tang and I. Johannsen, *Science*, 1998, **281**, 531.
49 J. P. Rabe and S. Buchholz, *Phys. Rev. Lett.*, 1991, **66**, 2096.
50 A. Stabel, R. Heinz, F. C. De Schryver and J. P. Rabe, *J. Phys. Chem.*, 1995, **99**, 505.
51 A. Gesquière, M. M. Abdel-Mottaleb, S. De Feyter, F. C. De Schryver, M. Sieffert, K. Müllen, A. Calderone, R. Lazzaroni and J.-L. Brédas, *Chem. Eur. J.*, 2000, **6**, 3739.
52 F. Stevens and T. P. Beebe, *Langmuir*, 1999, **15**, 6884.
53 M. M. S. Abdel-Mottaleb, S. De Feyter, A. Gesquière, M. Sieffert, K. Müllen and F. C. De Schryver, *Nano Letters*, 2001, **1**, 353.
54 P. C. M. Grim, S. De Feyter, A. Gesquière, P. Vanoppen, M. Rücker, S. Valiyaveettil, G. Moessner, K. Müllen and F. C. De Schryver, *Angew. Chem., Int. Ed. Engl.*, 1997, **36**, 2601.
55 S. W. Hla, G. Meyer and K.-H. Rieder, *Chem. Phys. Chem.*, 2001, **2**, 361.
56 Y. Okawa and M. Aono, *Nature*, 2001, **409**, 683.
57 A. Semenov, J. P. Spatz, M. Möller, J.-M. Lehn, B. Sell, D. Schubert, C. H. Weidl and U. S. Schubert, *Angew. Chem. Int. Ed.*, 1999, **38**, 2547.
58 U. Ziener, J. M. Lehn, A. Mourran and M. Möller, *Chem. Eur. J.*, 2002, **8**, 951.
59 M. M. S. Abdel-Mottaleb, N. Schuurmans, S. De Feyter, J. van Esch, B. L. Feringa and F. C. De Schryver, *Chem. Commun.*, 2002, 1894.